scientific reports

Check for updates

OPEN

GLUT1-mediated HMGB1 O-GlcNAcylation drives hyperglycemia-Induced neutrophil extracellular trap networks formation via TLR4 signaling and exacerbates fibroblast inflammation

Weijing Sun[1,3], Jinlong Xu[2,3], Shijie Li[1], Yue Zhao[1], Jiachen Fu[1], Lixia Di[1] & Dezhi Han[1]✉

Neutrophil extracellular traps (NETs) exacerbate fibroblast inflammatory injury in hyperglycemic conditions, yet the role of glucose metabolism and O-linked N-acetylglucosamine (O-GlcNAc) glycosylation in this process remains unclear. Here, we investigate how glucose transporter protein 1 (GLUT1)-dependent glucose uptake regulates O-GlcNAcylation of high-mobility group box 1 (HMGB1) to drive NET formation and fibroblast inflammation. Mouse peripheral blood neutrophils (MPBN) were treated with high glucose (25 mM) and phorbol ester (PMA) to induce NETs. Co-culture of NETs with mouse fibroblasts (L929) reduced fibroblast viability by 1.1 fold and migration by 1.2 fold within 24 h, while upregulating pro-inflammatory cytokines (Tumor Necrosis Factor-α (TNF-α): +1.3-fold; Interleukin-1β (IL-1β): +1.1-fold; Interleukin-6 (IL-6): +1.1-fold) and suppressing collagen synthesis (Collagen I (COL-I): − 1.7-fold; Collagen III (COL-III): −2.5-fold). Critically, high glucose elevated GLUT1 expression in MPBN (+ 1.2-fold), further amplified under co-culture conditions(+ 1.2-fold). Functional assays using GLUT1 knockdown confirmed that GLUT1 activity was essential for glucose uptake and subsequent O-GlcNAc modification of HMGB1, stabilizing its expression. Enhanced O-GlcNAcylation of high-mobility group box 1 (HMGB1) directly promoted NET formation, evidenced by elevated markers (Citrullinated histone H3 (Cit-H3): +1.6-fold; Myeloperoxidase (MPO): +1.2-fold; Circulating free DNA (cfDNA): +2-fold) and activation of c-Jun N-terminal kinase (JNK)/p38 phosphorylation. These effects were abolished by toll-like receptor 4 (TLR4) inhibition, linking HMGB1-TLR4 signaling to NET-driven inflammation. Mechanistically, GLUT1 knockdown reduced HMGB1 O-GlcNAcylation and reversed NET-induced fibroblast dysfunction. Our findings provide direct evidence that hyperglycemia enhances GLUT1 expression and activity, driving HMGB1 O-GlcNAcylation to maintain NETs formation through TLR4, which promotes fibroblast inflammatory injury. This pathway highlights a metabolic-inflammation axis relevant to diabetic complications.

Keywords Fibroblasts, GLUT1, HMGB1, Neutrophil extracellular trap network, O-GlcNAc glycosylation

Diabetes mellitus is a chronic metabolic disease with a global prevalence that causes serious complications. According to incomplete statistics, there are approximately 463 million people with diabetes worldwide. Of these, about 6.3% have diabetic foot ulcers and other diabetic traumatic lesions. The incidence of diabetic foot ulcers is even higher in China[1–3]. Diabetic wounds are a common chronic complication of diabetes mellitus.

[1]Department of Burn and Plastic Surgery, No. 969 Hospital, Joint Logistics Support Force of the Chinese People's Liberation Army, Hohhot City, China. [2]No. 969 Hospital, Joint Logistics Support Force of the Chinese People's Liberation Army, Hohhot City, China. [3]Weijing Sun and Jinlong Xu contributed equally to this work. ✉email: wound2024@163.com

They are stimulated by persistent hyperglycaemia and prolonged hypoxia, leading to problems such as skin ulceration, tissue necrosis, and wound infections. These issues can seriously affect the quality of life of patients and may even lead to disability and death[4]. During the initial stages of wound healing, the wound is primarily infiltrated by neutrophils, which serve a defensive and reparative function. However, an overabundance of neutrophils in the local area can have negative effects and hinder the wound healing process[5,6]. Neutrophils are primarily eliminated from the wound through apoptosis. However, they can also undergo neutrophil extracellular trapping network death (NETosis), a process in which activated neutrophils trap and kill pathogens by releasing neutrophil extracellular trap networks (NETs) outside the cell. These NETs consist of depolymerised chromatin and intracellular granule proteins[7]. NETs are network-like structures composed of free DNA, histones, antimicrobial peptides, and various granzymes that are released extracellularly by neutrophils. They function to restrict, trap, and kill pathogens, thereby preventing infections. However, excessive formation of NETs can also lead to tissue damage, which has been implicated in various diseases such as arteriovenous thrombosis and autoimmune diseases[8,9]. Research has demonstrated that the production of NETs is elevated in the wound tissue of diabetic patients and is positively associated with blood glucose concentration[10]. The hyperglycemic environment in diabetic patients creates a suitable habitat for pathogenic bacteria to thrive. This environment stimulates neutrophils to produce NETs, which may cause damage to wound tissue and impede healing. The mechanism behind this phenomenon has not yet been fully understood.

O-GlcNAc (O-Linked N-Acetylglucosamine) glycosylation is a dynamic protein post-translational modification widely found in eukaryotes. It is a reversible monosaccharide modification catalyzed by O-GlcNAc glycosyltransferase (OGT), and its glycosylation occurs in cytoplasmic and nuclear protein serine (Ser)/threonine (Thr) residues[11]. Studies have shown that OGT-mediated O-GlcNAcylation modification can affect protein catalytic activity, subcellular localization, and interaction with other proteins, and is involved in a variety of biological processes, including cell growth and morphogenesis, metabolism, apoptosis, and transcriptional regulation[12]. O-GlcNAc glycosylation modification usually interacts with serine/threonine phosphorylation modification or modifies successively. O-GlcNAcylation can often improve the stability of the target protein and maintain its high expression status[13]. Balana et al.reported that HMGB1 has O-GlcNAc glycosylation modification, mainly at the S100 modification site. The O-GlcNAc glycosylation modification of HMGB1 weakens its ability to bind to DNA[14]. However, what biological functions it mediates remains to be elucidated.

GLUT1 is widely distributed in human tissues and cells and is the main carrier of glucose transport. Glucose molecules enter the cell through GLUT1 to be phosphorylated into glucose-6-phosphate. This molecule is then further catabolised into metabolites such as pyruvate and lactate via the glycolytic pathway[15]. GLUT1 supplies cells with the substrates necessary for glycolysis. The expression level of GLUT1 in neutrophils is closely related to its activity. Changes in GLUT1 expression may affect the immune function and metabolic status of neutrophils, which in turn affects the release of NETs[16]. O-GlcNAc (O-Linked N-Acetylglucosamine) glycosylation is a dynamic post-translational modification of proteins that is widely found in eukaryotes. Glucose can provide a substrate for glycosylation modification. Glucose can serve as a substrate for this modification. The level of O-GlcNAc modification is increased by highly expressed GLUT1 through the hexosamine biosynthetic pathway (HBP). However, it is unclear whether GLUT1 plays a significant role in the formation and release of NETs in neutrophils induced by high glucose. In diabetic wounds, persistent hyperglycemia disrupts neutrophil apoptosis and promotes NETosis, leading to excessive NETs that impair fibroblast function—a critical cell type for collagen synthesis and wound closure[17,18]. Recent studies suggest that metabolic reprogramming via GLUT1 in neutrophils may exacerbate NET-driven inflammation, but the role of glucose flux and O-GlcNAcylation in this axis remains unexplored[19,20]. This project aims to investigate the regulation of immune cell-fibroblast crosstalk under high glucose-induced conditions, and to reveal the molecular mechanisms involved in the regulation of O-GlcNAc glycosylation modification and NETs release by GLUT1.

Results

High glucose environment promotes fibroblast inflammatory response and wound healing disorder

To investigate whether a high glucose (25mM) environment induces inflammatory damage to fibroblasts through NETs. First, we used high glucose (HG) to treat neutrophilic granulocyte (HG + PMA-), and used NETs inducer phorbol-12-myristate-13-acetate (PMA) as a positive control (HG-PMA+). At the same time, in order to promote the further formation of NETs, neutrophils were treated with high glucose and PMA (HG + PMA+). As expected, compared with the control group, the levels of cfDNA, MPO, and Cit-H3 in the HG + PMA-group increased by 58.4 times, 2.9 times, and 3.3 times, respectively. The levels of cfDNA, MPO and Cit-H3 in the high glucose culture group (HG + PMA+) were 1.6 times, 1.3 times and 1.3 times higher than those in the normal culture group (HG-PMA+), respectively. Compared with the HG + PMA-group, the cfDNA level of the HG + PMA + group increased by 2.3 times, the Cit-H3 increased by 1.8 times, and the MPO increased by 2.1 times .High glucose combined with PMA further promoted the formation of NETs (Fig. 1a). This indicates that we successfully formed NETs by high glucose and PMA treatment. Fibroblasts play an important role in supporting wound healing. Therefore, we then explored the effect of NETs on the function of fibroblasts. We extracted the neutrophil suspension of HG + PMA + group to produce NETs for further study. CCK8 assay showed that compared with the normal culture group (control group), fibroblasts treated with NETs (HG group) showed a significant decrease in cell viability by 1.1 times in the presence of high glucose medium. L929 cells treated with high glucose medium alone had no significant effect on cell viability(Fig. 1b-c). Subsequently, Scratch and transwell experiments were used to evaluate the migration ability of fibroblasts. Compared with the normal culture group (control group), the migration ability of fibroblasts treated with NETs (HG group) decreased by more than 1.2 times in the case of high glucose medium culture. (Fig. 1d-e). These results indicate that in a high glucose environment, the viability and migration ability of fibroblasts treated with NETs are inhibited. In view

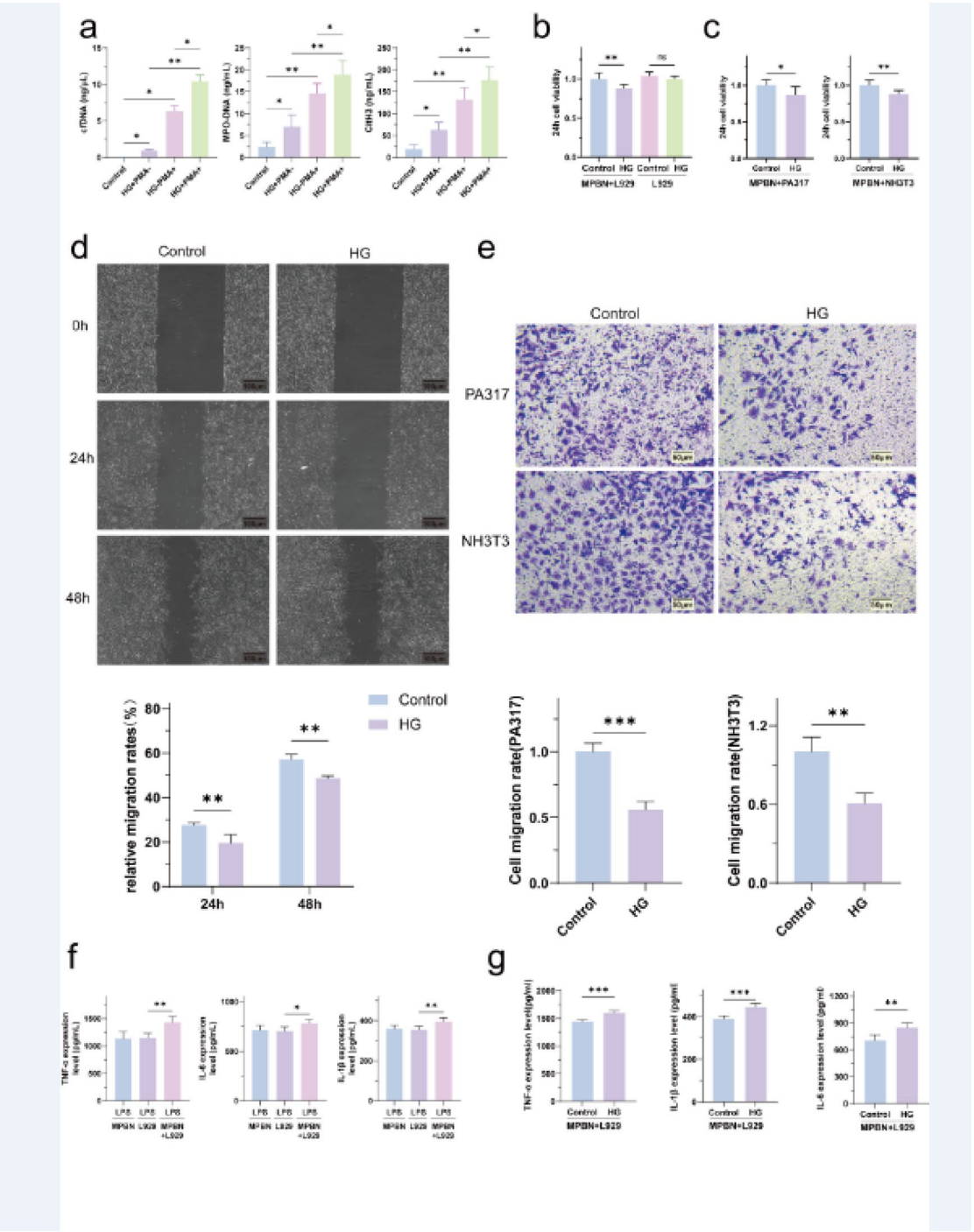

Fig. 1. Detection of cell activity, migration level and inflammatory factor secretion. (**a**) The effect of high glucose environment on NETs formation (cfDNA, MPO, Cit H3 content) was determined by free DNA quantification and ELISA. (**b**–**c**) CCK8 assay to detect cell activity in Control co-culture group, HG co-culture group, Control group, HG group. (**d**, **e**) Scratch and Transwell assay to evaluate cell migration level. (**f**) ELISA was used to detect the content of inflammatory factors in normal glucose concentration culture and LPS-induced MPBN, L929 and MPBN + L929 co-culture. (**g**) ELISA method to detect TNF-α, IL-1β and IL-6 expression levels. $^{*}P < 0.05$, $^{**}P < 0.01$, $^{***}P < 0.001$. $n = 3$, the experiment was repeated 3 times. NETs, Neutrophil extracellular traps; cfDNA, Circulating free DNA; MPO, Myeloperoxidase; Cit-H3, Citrullinated histone H3; CCK8, Cell Counting Kit-8; LPS, Lipopolysaccharide; TNF-α, Tumor Necrosis Factor-α; IL-1β, Interleukin-1β; IL-6, Interleukin-6.

of the pro-inflammatory effect of NETs, we detected inflammatory factors, Tumor Necrosis Factor-α (TNF-α), Interleukin-1β (IL-1β), Interleukin-6 (IL-6). Both L929 and MBPN cells produce inflammatory factors. In order to distinguish the production of inflammatory factors in untreated and glucose-treated cells, we analyzed the content of inflammatory factors after adding Lipopolysaccharide (LPS) to cells alone or in co-culture. The results showed that the content of inflammatory factors produced under co-culture conditions increased significantly (more than 1.1-fold) (Fig. 1f). The content of inflammatory factors in high glucose environment was further analyzed. Similarly, compared with the control group, the content of inflammatory factors in the HG group increased by more than 1.1 fold. (Fig. 1g). These results suggest that NETs promote the production of inflammatory factors in a high glucose environment. Furthermore, the collagen secretion level of fibroblasts was observed through immunofluorescence staining. It was found that compared with the normal culture group, the protein secretion levels of Collagen I (COL-I) and Collagen III (COL-III) in L929 cells inhibited by MBPN were more than 1.7 times under high glucose-induced conditions (Fig. 2a, b). The secretion of COL-I and COL-III by fibroblasts is related to wound healing. Elevated levels of their secretion usually reflect tissue repair or remodeling. This indicates that NETs may decrease wound repair ability in high glucose environment. RT-qPCR results showed that the mRNA levels of COL-I and COL-III in HG group were significantly higher(+1.6-fold) than those in control group (Fig. 2c). These results indicate that NETs promote fibroblast inflammatory response and hinder wound healing in high glucose environment.

Glucose transporter 1(GLUT1) drives O-GlcNAc glycosylation modification of high-mobility group box 1(HMGB1) and upregulates HMGB1 expression

As the main carrier of glucose transport, GLUT1 expression affects the formation and release of neutrophil NETs. Therefore, we determined the expression of GLUT1 in high glucose environment. The results showed that compared with the Control group, the expression of GLUT1 in the HG group was significantly increased(+1.2-fold). In the co-cultured cells of MPBN and L929, GLUT1 in the HG group was also significantly highly expressed(+1.2-fold). We further successfully constructed neutrophils overexpressing GLUT1 and co-cultured them with L929 cells. The results showed that more GLUT1 was expressed(+2-fold) after co-culture, and the expression of GLUT1 was the highest(+1.1-fold) in high glucose environment. At the same time, when the expression of GLUT1 was silenced, the expression of GLUT1 in the high glucose environment was still higher (+4.2-fold) than that in the normal environment (Fig. 3a). These results suggest that GLUT1 expression is indeed increased in co-cultured cells under high glucose conditions. HMGB1 can delay skin wound healing by promoting the formation of NETs, while HMGB1 has O-GlcNAc glycosylation modification. In high glucose environment, the expression of GLUT1 in fibroblasts treated with NETs was increased. Therefore, we used Co-IP experiment to detect the expression of HMGB1 and the level of O-GlcNAc glycosylation modification after MPBN overexpression of GLUT1 in high glucose environment, and added OGA inhibitor ThiametG (TMG) intervention. It was found that overexpressing GLUT1 led to a significant up-regulation of the level of O-GlcNAc glycosylation modification of HMGB1. Low expression of GLUT1 showed the opposite effect. When glycosyl hydrolase OGA was used as an intervention, the O-GlcNAcylation level of HMGB1 was further up-regulated, along with an increase in the protein level of HMGB1 (Fig. 3b). This indicates that overexpression of GLUT1 increases the glycosylation modification of HMGB1 in high glucose environment, thereby improving the stability of HMGB1 protein.

HMGB1 mediates the formation and release of NETs through the toll-like receptor 4(TLR4)/mitogen-activated protein kinase (MAPK) pathway.

The formation of neutrophil NETs induced by HMGB1 is related to TLR4. The activation of TLR4 affects the MAPK signaling pathway. In order to explore the effects of HMGB1 and GLUT1 on TLR4 and MAPK signaling pathways in high glucose environment, we first used immunofluorescence to analyze the effects of HMGB1 on neutrophils and the formation of NETs after overexpression of GLUT1 in neutrophils. At the same time, we analyzed whether the use of TLR4 inhibitor (TAK-242) affected the formation of NETs. These groups of cells were treated with PMA in a high glucose environment. The results showed that compared with the HG group, the fluorescence density of Cit-H3 and MPO increased (+1.3-fold, 1.5-fold) after HMGB1 intervention in neutrophils, and increased significantly (+1.8-fold, 2.2-fold) after overexpression of GLUT1. However, the fluorescence density of Cit-H3 and MPO decreased (-2.5-fold, 3.7-fold) after the use of TAK-242 and GLUT1 knockdown expression (Fig. 4). We further analyzed the concentrations of cfDNA, Cit-H3 and MPO in cell culture medium (Fig. 5a). This indicates that HMGB1 does promote the formation of NETs, and overexpression of GLUT1 also promotes the formation of NETs, while inhibiting the expression of TLR4 is weakened, which is the same as the expected results. In order to further analyze the mechanism of NETs release, we detected the phosphorylation levels of JNK and p38 proteins. The results showed that the phosphorylation levels of JNK and p38 proteins changed at 2 h, but the results were not significant. After 4 h and 6 h, the phosphorylation levels of JNK and p38 proteins in HMGB1 intervention and GLUT1 overexpression groups were significantly increased (more than 1.3-fold, 1.8-fold), while the TAK-242 group was significantly reduced (more than 1.6-fold, 2-fold). The prolonged time course showed a small but significant enhancement/reduction effect between 2 and 6 h (Fig. 5b). The results indicate that HMGB1 promotes the formation and release of NETs through the TLR4/JNK/p38 MAPK pathway.

Discussion

In this study, we revealed a new mechanism for the formation of neutrophil NETs in diabetic wounds. Our findings indicate that the formation of neutrophil NETs is promoted in high glucose environment, while excessive NETs aggravate inflammatory injury of fibroblasts and hinder wound healing process. Under high glucose conditions, GLUT1 expression in neutrophils was up-regulated, and overexpression of GLUT1 further enhanced

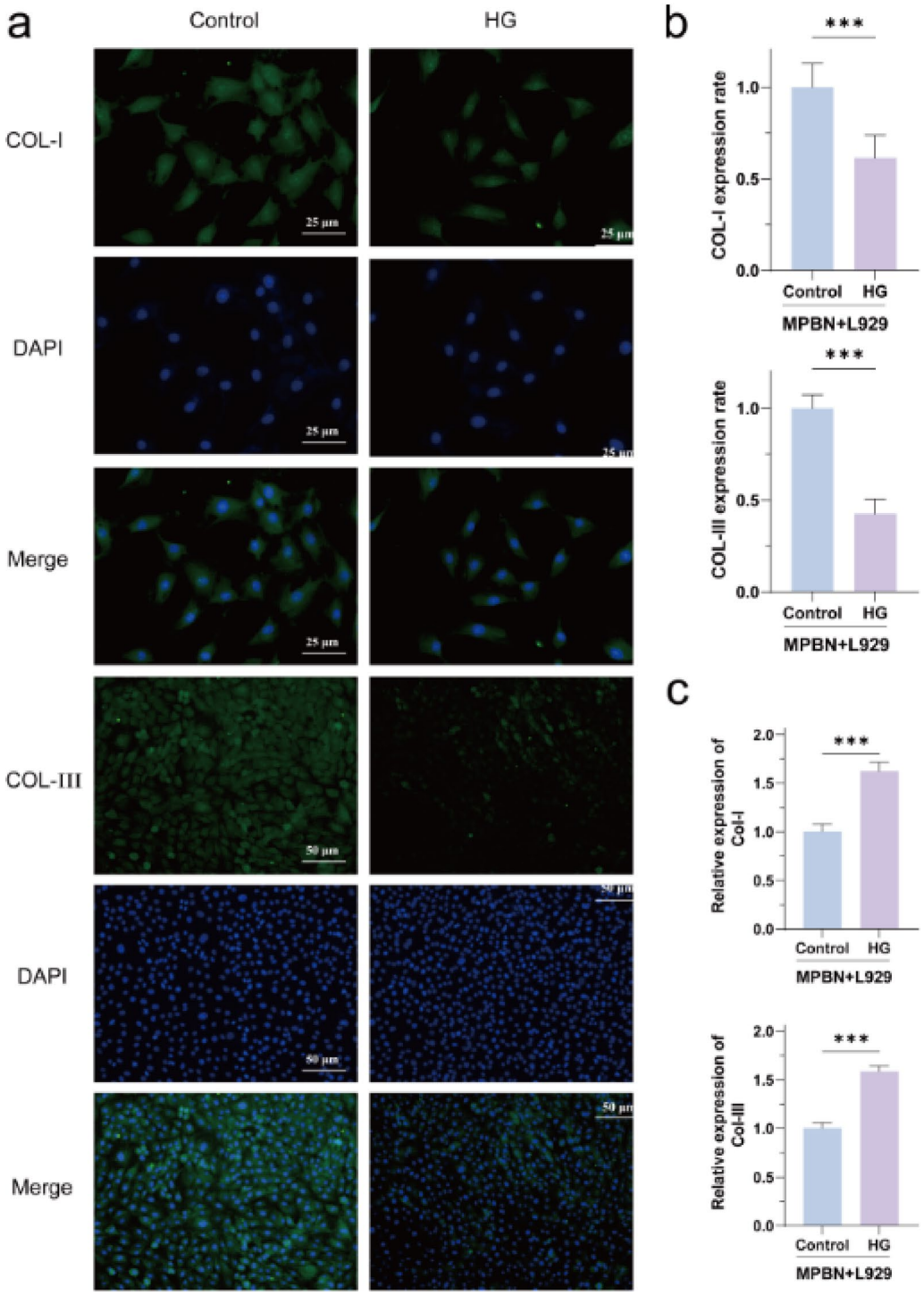

Fig. 2. Detection of cellular collagen component expression. (**a**, **b**) Detection of COL-I and COL-III expression levels by immunofluorescence staining. (**c**) RT-qPCR was used to detect the content of COL-I and COL III collagen mRNA in the co-culture group. ***$P < 0.001$. $n = 3$, the experiment was repeated 3 times. COL-I, Collagen I; COL-III, Collagen III.

high glucose-induced O-GlcNAcylation of HMGB1 and its expression level. We confirmed that HMGB1 and GLUT1 can promote the formation of NETs, while the inhibition of TLR4 can weaken the formation of NETs. In addition, HMGB1 further affects the formation of NETs by regulating the expression of TLR4 / MAPK signaling pathway-related proteins.

Diabetes mellitus, a condition characterized by inflammatory or metabolic factors such as hyperglycemia, can increase neutrophil activation and the production of NETs[17,21]. Abnormal NETs may impede diabetic healing. The role of GLUT1 in regulating collective immune function is well known, but its molecular mechanism

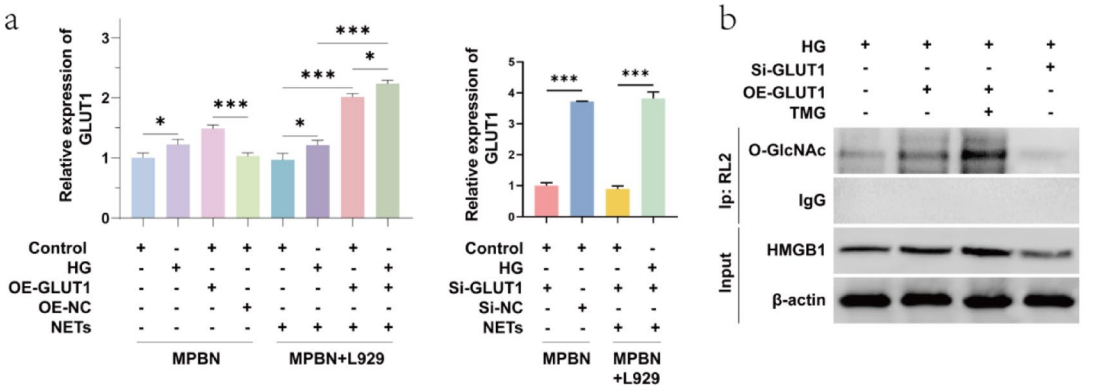

Fig. 3. Detection of cellular GLUT1 and O-GlcNAc modified HMGB1 levels. (**a**) RT-qPCR to detect cellular GLUT1 mRNA levels in each group. (**b**) Co-IP detection of O-GlcNAc-modified HMGB1 levels. ***$P < 0.001$. $n = 3$, the experiment was repeated 3 times. GLUT1, Glucose transporter 1; HMGB1, High-mobility group box 1.

in neutrophil activation and inflammatory response is unclear. In our study, high glucose did promote the formation of NETs in MPBN cells, such as the significant increase of MPO and Cit H3. Next, we co-cultured the neutrophil suspension that successfully produced NETs with fibroblasts to detect the effect of NETs on the function of fibroblasts. Consistent with the reported results, the proliferation and migration of fibroblasts were significantly reduced in high glucose environment. At the same time, the levels of inflammatory factors (TNF-α, IL-1β, and IL-6) also increased, the immunofluorescence density of COL-I and COL-III decreased, and mRNA expression increased. In Chu et al. ' s study, the proliferation and migration of fibroblasts induced by high glucose were decreased after treatment with high concentration of NET[21]. Fibroblast proliferation, migration, and collagen synthesis are crucial indicators of the wound healing process. This further proves that excessive NET inhibits wound healing by impairing the function of fibroblasts and inflammatory damage in diabetic high glucose environment.

The microenvironment with high glucose levels in diabetic patients leads to a significant increase in protein O-GlcNAc glycosylation modifications. In the diabetic state, one of the mechanisms by which hyperglycemia promotes the inflammatory process is the abnormally elevated protein O-GlcNAcylation. Li et al.[16] discovered that neutrophils increase glucose uptake by expressing GLUT1. In mice with neutrophil-specific knockout GLUT1, there was an increase in mortality from candidiasis due to impaired neutrophil phagocytosis, reactive oxygen species, and extracellular trap formation. GLUT1 facilitates the process of protein O-GlcNAcylation by providing substrates for glycosylation modifications[22]. Our study found. In the high glucose environment, the expression of GLUT1 in MPBN increased, and when GLUT1 was overexpressed, the level of O-GlcNAc protein increased. After the addition of TMB, the level of O-GlcNAc protein increased further. In the introduction, we mentioned that GLUT1 increased the level of O-GlcNAc modification, which was consistent with our research results. At the same time, because HMGB1 can promote the formation and release of neutrophil NETs[23,24], and HMGB1 has O-GlcNAcylation modification[25]. In addition, HMGB1 can target innate immune signals, leading to autoimmune and sterile damage. And as a damage-associated molecular pattern (DAMP) to promote the formation and release of NETs[24,26]. Therefore, we detected the levels of HMGB1 and O-GlcNAc glycosylation in high glucose environment. As expected, overexpression of GLUT1 increased the expression of HMGB1 in high glucose environment, and O-GlcNAcylation maintained the stability of the target protein. As the target protein of O-GlcNAc glycosylation, the expression of HMGB1 is increased. Our study showed that high glucose environment promoted the expression of GLUT1 in neutrophils, while GLUT1 promoted the O-GlcNAcylation of HMGB1 and maintained the stability of HMGB1 protein.

Studies have shown that HMGB1-induced neutrophil extracellular traps (NETs) formation depends on the interaction with TLR4. It was found that the deletion of HMGB1 weakened the ability of neutrophils to produce NETs, while the deletion of TLR4 further reduced the formation of NETs[23]. In our study, the use of TLR4 inhibitor TAK-242 did significantly reduce the content of MPO, Cit H3, and cfDNA. In addition, Kazuya et al.showed that TLR4 activation can induce nuclear factor kappa-B (NF-κB) and MAPK signaling pathways and play a key role in regulating IL-6 mRNA stability[27]. In the study of Zhou et al., TLR4-MyD88-MAPK signaling pathway plays a role in regulating mTOR-dependent autophagy and inhibiting intestinal inflammation and oxidative stress injury[28]. Therefore, we examined the MAPK signaling pathway-related proteins in neutrophils under HMGB1 intervention and GLUT1 overexpression. We showed the changes of signaling pathway-related proteins in a time-dependent manner. The results showed that the expression of these proteins increased significantly under HMGB1 intervention and GLUT1 overexpression conditions, but decreased after inhibition of TLR4. In this study, we verified the key role of GLUT1 activity in HMGB1 O-GlcNAcylation by GLUT1 knockdown experiments, and found that HMGB1 O-GlcNAcylation directly promoted the up-regulation of NETs markers (Cit-H3, MPO, cfDNA) and the activation of TLR4 / MAPK signaling pathway by stabilizing its protein expression level. In addition, the use of TLR4 inhibitor TAK-242 significantly weakened the formation

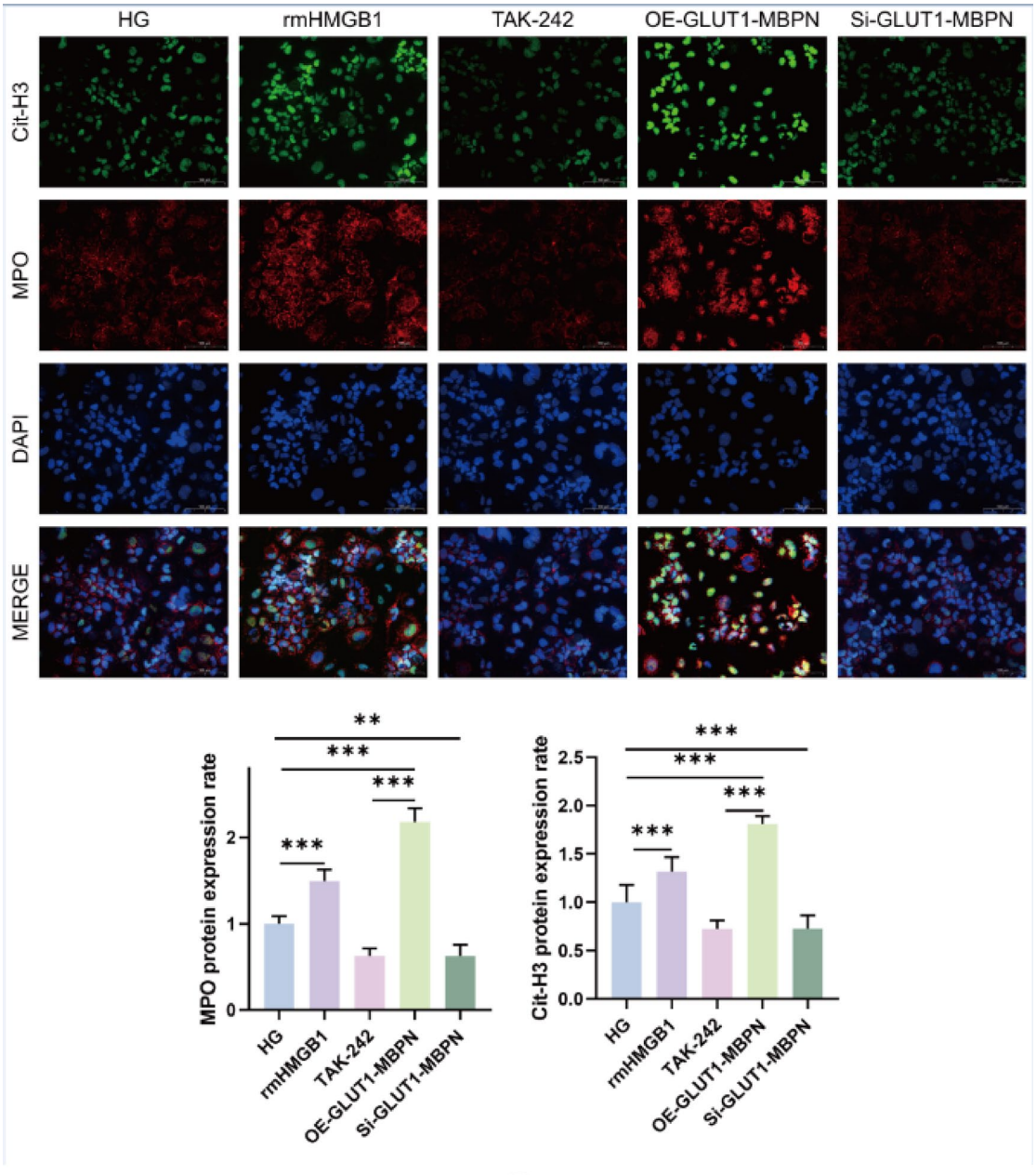

Fig. 4. Immunofluorescence staining of Cit-H3, MPO expression levels to assess NETs formation. $^{*}P < 0.05$, $^{**}P < 0.01$, $^{***}P < 0.001$. $n = 3$, the experiment was repeated 3 times.

of NETs and its inhibitory effect on fibroblast function. These results indicate that O-GlcNAcylation plays an important role in NETs formation and fibroblast inflammatory injury through HMGB1-TLR4 signaling pathway. Therefore, we speculate that in the diabetic high glucose environment, up-regulated GLUT1 maintains the protein stability of HMGB1 by mediating the O-GlcNAcylation of HMGB1, and promotes the formation of neutrophil NETs by regulating the TLR4/MAPK signaling pathway. Produce inflammatory factors, thereby hindering fibroblast wound healing.

In summary, we have shown that in a high-glucose environment, up-regulation of GLUT1 expression promotes O-GlcNAc glycosylation modification of HMGB1, which enhances protein stability. This, in turn, contributes to the formation and release of NETs, promoting inflammatory responses in fibroblasts. However, it is important to note that this study has limitations. For instance, the use of mouse models to intervene in the GLUT1 and HMGB1 glycosylation modification process needs to be validated to probe the effects on diabetic wound healing. This study found a new mechanism of diabetic wound healing, which may provide new ideas and potential therapeutic targets for the clinical treatment of diabetes.

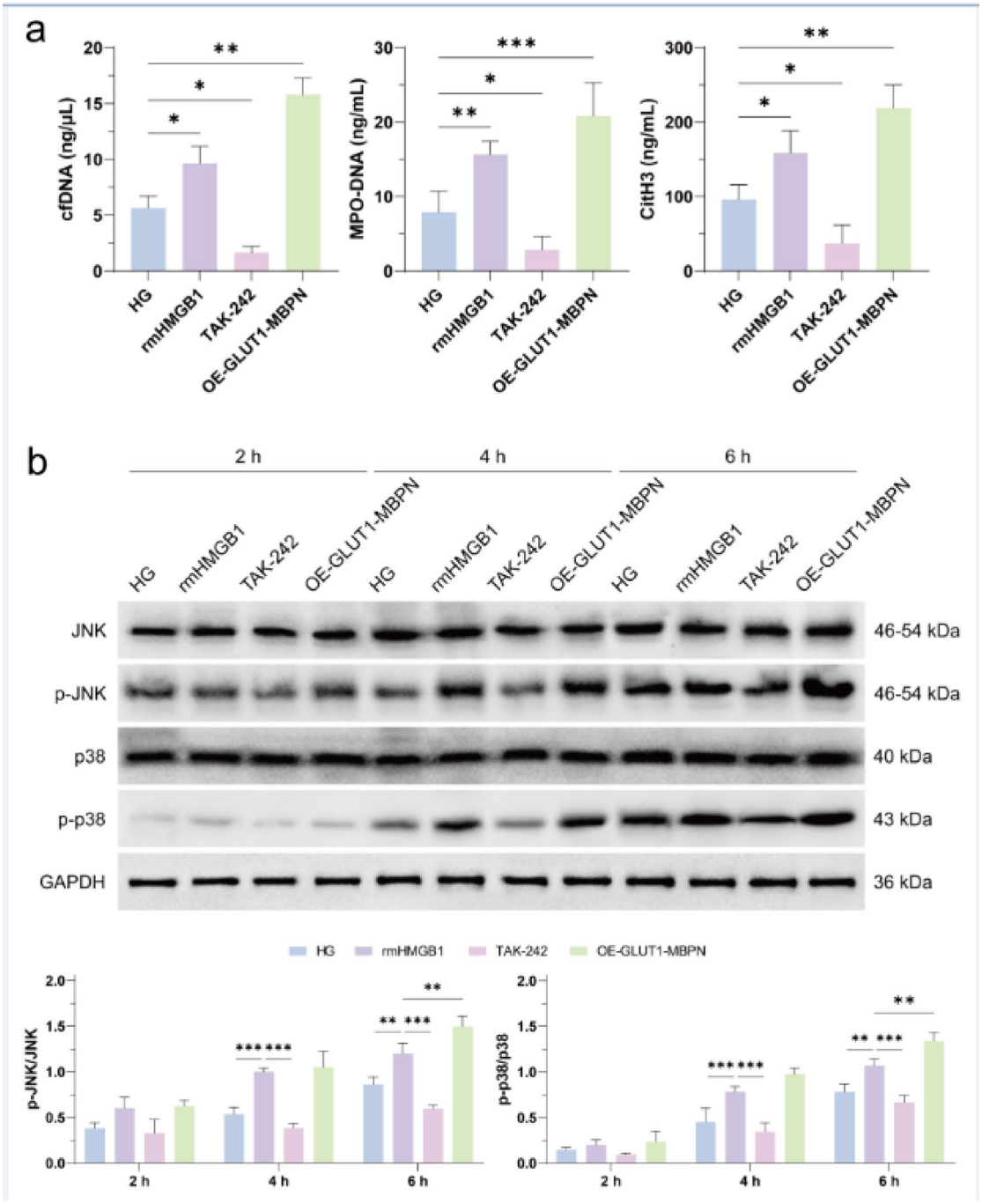

Fig. 5. Detection of NETs-related molecules, JNK/p38 MAPK signalling pathway expression. (**a**) Free DNA quantification and ELISA to detect cfDNA, MPO-DNA and Cit-H3 expression levels. (**b**) The phosphorylation level of JNK, p-38 protein was determined by western blot. $^{*}P<0.05$, $^{**}P<0.01$, $^{***}P<0.001$. $n=3$, the experiment was repeated 3 times. JNK, c-Jun N-terminal kinase; MAPK, mitogen-activated protein kinase; p, phosphorylated.

Materials and methods

Materials

Fetal bovine serum (FSD500) (Excell Bio, China). Penicillin-streptomycin solution (100X) (C0222) (Beyotime, China). RPMI 1640 medium (11875093) (Gibco, China). DMEM High Sugar Medium (11965118), Trypsin (R001100) (Gibco, China). Cell Freezing Solution (C0210B-50 ml), PBS Buffer (C0221A) (Beyotime, China). Cell/Tissue Total RNA Isolation Kit V2 (RC112), HiScript lll 1st Strand cDNA Synthesis Kit (R312), Taq Pro Universal SYBR qPCR Master Mix (Q712) (Vazyme, China). OE- GLUT1 and its NC plasmid (Shanghai Genechem Co.,Ltd., China). LipofectamineTM 3000 (L3000015) (Thermo Fisher, USA). 30% Acr/Bic (BL513A), Tris-Base (BS083), TBS buffer (BL602A) (Biosharp, China). BSA protein standard (BL673A), Tween-20 (BS100)

(Biosharp, China). SDS (3250), Glycine (1275), Skimmed milk (1172) (BioFroxx, China). BCA protein Content Assay Kit (WB6501), 5xSDS-PAGE Sampling Buffer (WB2001), ECL Luminescent Solution AB (P2100) (NCM Biotech, China). Prestained Protein Marker II (G2058-250UL) (Servicebio, China). Western Antibody Diluent (C05-07001), Goat Anti-Rabbit IgG H&L/HRP (bs-0295G-HRP) (C05-07001), Goat Anti-Mouse IgG H&L/HRP (bs-0296G-HRP) (Bioss, China). SAPK/JNK Antibody #9252, Phospho-SAPK/JNK (Thr183/Tyr185) (81E11) Rabbit mAb #4668, p38 MAPK Antibody #9212, Phospho-p38 MAPK (Thr180/Tyr182) (D3F9) XP® Rabbit mAb #4511 (CST, USA). Anti-O-linked N-acetylglucosamine antibody, clone RL2 (MABS157), 1% crystal violet (V5265-250ML) (Sigma Aldrich, USA). Anti-GAPDH antibody [6C5] - Loading Control (ab8245), Anti-HMGB1 antibody (ab18256), Anti -Collagen I antibody [EPR24331-53] (ab270993), Anti-Collagen III antibody [EPR17673] (ab184993), Anti-Histone H3 (citrulline R2 + R8 + R17) antibody [RM1001] (ab281584), Anti-Myeloperoxidase antibody [EPR20257] (ab208670) (Abcam, UK). O-GlcNAc Antibody (RL2) - BSA Free (NB300-524) (Novus, USA). Alexa Fluor™ 488 (A21206) and Alexa Fluor™ 546 (A21447) (Invitrogen, USA). CCK8 Cell Proliferation Detection Kit (BA00208) (Bioss, China). Mouse Peripheral Blood Neutrophil Isolate Kit (P9201), Free DNA Extraction Kit(D1810) (Solarbio, China). Mouse TNF-α ELISA Kit (PT512), Mouse IL-6 ELISA Kit (PI326) (Beyotime, China). Mouse IL-1β (Interleukin 1 Beta) ELISA Kit (E-EL-M0037) (Elabscience, China). Triton X-100 (P0096), 4% paraformaldehyde (P0099-500 ml), DAPI (C1006) (Beyotime, China). Sealed Goat Serum (10%) (C01-03001) (Bioss, China). Thiamet G (HY-12588), HMGB1/HMG-1 Protein, Mouse (HY-P73104), Resatorvid (TAK-242) (HY-11109) (medchemexpress, USA). Mouse Myeloperoxidase-DNA complex (MPO-DNA) ELISA kit (HB1200-Mu) (Hnybio, China). Mouse citrullinated histone H3 (CITH3) ELISA kit (ml058746) (Mlbio, China). Quant-iT PicoGreen dsDNA Assay Kits (P7589) (ThermoFisher). Transwell chamber (8 μm model: 3422) (CORNING, China).

Experimental apparatus

Real-time fluorescence quantitative PCR instrument CFX96 Touch 1,855,195, Western blotting system (model: Criterion™ electrophoresis tank, Trans-blot® transfer tank) (Bio-Rad, USA). Attune NxT Flow Cytometer (Themo Fisher, USA). EVOS M5000 fluorescence microscope (Themo Fisher, USA). Optical microscope (Shanghai Optical Instrument No.1 Factory, China). JP-K6000 chemiluminescence analyzer, Ultramicro nucleic acid protein analyzer Nano-600 (Shanghai Jiapeng, China). Ultra-low temperature refrigerator (Haier, China). 10T Transfection kit (Nanjing Jiangyuan Biotechnology Co., Ltd., China). Multiskan FC microplate reader 357-714018(Thermo Fisher Scientific, USA).

Cell culture and stimulation

The experimental procedures were in accordance with The 969th Hospital of the joint logistics support force of P.L.A Laboratory Animal Ethics Committee Regulations. All methods were performed in accordance with relevant guidelines and regulations and in accordance with ARRIVE guidelines. C57BL/6 wild-type mice were procured from Guangdong Laidi Biomedical Research Institute Co., Ltd. (SYXK 2022 – 0296). C57BL/6 WT mice were rendered anaesthetized through the administration of sodium pentobarbital (35 mg/kg body weight). Subsequent to the administration of anesthesia, the abdominal skin was prepared along the midline. The abdominal aorta was identified by peeling back the intestines and other abdominal organs with a cotton swab after the abdomen has been opened. Subsequently, a needle was inserted into the abdominal aorta for the purpose of collecting blood. The objective was to collect blood from the mice in order to extract neutrophils. After completing the blood collection, the mice were euthanized by cervical dislocation. In accordance with the instructions provided in the kit for the extraction of mouse peripheral blood neutrophils, the neutrophil layer was obtained by taking 5mL of fresh anticoagulated whole blood and adding the reagents as per the kit instructions. The mixture should then be subjected to centrifugation in order to separate the lower neutrophil layer. Subsequently, the cells should be washed and resuspended in PBS. The neutrophils were cultured in RPMI medium, which contained 1% penicillin-streptomycin, 2 mM L-glutamine, 25 mM HEPES, and 10% FBS. The temperature was maintained at 37 °C with 5% CO_2 in the incubator. To create the high-glucose induction model, neutrophils were cultured in a medium containing 25 mM glucose. The neutrophils were inoculated into 6-well plates at a density of 1×10^6 cells per well and stimulated with 100 nM PMA per well for four hours to induce the formation of NETs.

The L929 cells were cultured in DMEM culture base supplemented with 10% fetal bovine serum, penicillin (100 units/mL), and streptomycin (50 units/mL). Neutrophil suspensions forming NETs were added to L929 cells cultured in normal medium and incubated for 24 h to form a co-culture model (Control group). Neutrophil suspension forming NETs (High glucose and PMA co-culture, HG + PMA+) was added to L929 cells cultured in high glucose and incubated for 24 h to create a co-culture model (HG group). In MPBN cells, construction of HG groups was induced by 25 mM high glucose. The OE/Si-GLUT1 group was constructed by Lipofectamine 3000 reagent and infecting MPBN cells with lentiviral pLV-eGFP-N-Puro-OE/Si-GLUT1 expression vector viral solution, and the OE-GLTU1 + TMG group was constructed by treating the cells with 100μM OGA inhibitor ThiametG (TMG). 100ng/ml recombinant mouse HMGB1 intervened neutrophils for 6 h to construct rmHMGB1 group, and 2μM TLR4 inhibitor TAK-242 treated neutrophils to construct TAK-242 group. The cells in rmHMGB1 and TAK-242 groups were cultured in HG + PMA + medium.

CCK8 assay

L929, PA317, NH3T3 cells in logarithmic growth phase were inoculated into 96-well plates at a density of 2000 cells per well and incubated at 37 °C with 5% CO_2 for 4–8 h.After the cells were adherent, the NET neutrophil suspension was co-incubated with mouse fibroblasts or L929 alone for 24 h. The incubated cells were divided into Control group and HG group. Among them, the fibroblasts in the Control group were cultured in normal medium, and the HG group was cultured in medium containing 25 mM glucose. After the incubation was

completed, the culture medium was removed, washed with PBS, and CCK8 (10μL/well) was added to continue the incubation for 2 h. Finally, the optical density at 450 nm was detected by a microplate reader.

Cell scratch assay

Parallel lines at 0.5 cm intervals should be drawn on the back of the 6-well plate. Cells from each experimental group should be collected and inoculated at a density of 1×10^6 cells/well into the 6-well plate. When the cells have reached over 90% growth, draw parallel lines on the cells with the tip of the pipette gun. Photographs were taken under a microscope to record the size of the cell scratches at 0, 24 and 48 h.

Transwell assay

Transwell assay was used to evaluate the migration ability of other fibroblasts (PA317, NH373). The cells in the logarithmic growth phase were digested and resuspended in serum-free medium. The cell density was adjusted to 2×10^5 cells / mL and inoculated into the upper chamber of 24-well Transwell plate (100 μL/well). The lower chamber was added with 600 ul of medium containing 10% FBS.After 24 h, the upper membrane cells were washed off with PBS, and the cells migrated on the lower surface were stained with crystal violet crystal violet. After washing with PBS, the stained cells were counted by optical microscope.

Enzyme-linked immunosorbent assay (ELISA)

The supernatant of each group of L929 cells was obtained, and the standard was diluted according to the manufacturer's instructions of the Cit-H3, MPO, TNF-α, IL-6, and IL-1β ELISA kit. The sample was added 50 μl and incubated at 37 °C for 30 min. After washing, the enzyme-labeled reagent was added and the absorbance of each hole was measured at 450 nm.

CfDNA quantification

After the experimental intervention, the cell culture medium of each group was collected, centrifuged at 4℃ and 12,000 rpm for 10 min, and the supernatant was collected. The supernatant was centrifuged at 4 °C and 6000×g for 45 min using an ultrafiltration tube (10 kDa MWCO) to obtain a concentrated culture medium of about 65 μL. According to the manufacturer 's instructions, cfDNA in the concentrate was extracted using a free DNA extraction kit. Finally, the cfDNA concentration of each sample was measured at 260 nm using an ultra-micro nucleic acid protein analyzer Nano-600.

Immunofluorescence staining

MPBN were inoculated at a concentration of 1×10^6 cells/well in 6-well plates and cultured at 37 °C with 5% CO_2 for 24 h. Finally, the supernatants were discarded and the cells were washed with PBS. The cells were fixed with 1 ml of 4% paraformaldehyde. Then, they were permeabilized with 1 ml of 0.25% Triton-X100 (TBST) and blocked with 1 ml of goat serum. The cells were incubated with 1 ml of primary antibody (1:200) overnight at 4 °C. After washing with TBST, 1 ml of secondary antibody (1:200) was added and incubated. The cells were then stained with DAPI and photographed under a fluorescence microscope to observe the fluorescent expression of COL-I, COL-III, We calculated at least five different fields of view under each experimental condition, each field of view contains three non-overlapping regions, and a total of at least 15 combined fields.

RNA extraction and quantitative real-time polymerase chain reaction (qPCR)

The total cellular RNA was extracted using Trizol reagent. The purified RNA was obtained through chloroform phase separation, isopropanol precipitation, and 75% ethanol washing. The cDNA was obtained by preparing a reverse transcription system and reacting at 25 °C for 5 min, 42 °C for 30 min, and 85 °C for 5 min. A real-time quantitative PCR reaction system was prepared and the reaction was performed using the CFX96 Touch 1,855,195 Real-time Fluorescence Quantitative PCR Instrument. The following procedure were used: pre-denaturation at 95 °C for 30s, denaturation at 95 °C for 10s. Annealing at 60 °C for 10 s, extension at 95 °C for 15s, and cycle count of 40, melting curve: 60 °C for 60s, 95 °C for 15 s. The experimental results were calculated using $2^{-\Delta\Delta Ct}$. The primer sequences were as follows: GLUT1, forward 5'-ATCCATGGAGACCGCTTCAT-3', reverse 5'-CGT ATGTGCGTATGTGCGTATTG-3'; COL-I, forward 5'-TTCTCCTGGCAAAGACGGAC-3', reverse 5'-CTCAA GGTCACGGTCACGAA-3'; COL-II, forward 5'- GAGGAATGGGTGGCTATCCG-3', reverse 5'- TCGTCCAG GTCTTCCTGACT-3'; GAPDH, forward 5'-ACCACAGTCCATGCCATCAC-3', reverse 5'-TCACCACCCTGT TGCTGTA-3'.

Immunoprecipitation (IP)

MPBN cells were collected, cell lysis buffer was added, and the supernatant was centrifuged. 2 μg of antibody and 5 μL of protein A/G-beads were added to the cell lysate and incubated slowly at 4 °C overnight. After the immunoprecipitation reaction, protein A/G-beads were centrifuged at 4 °C. The supernatant was removed and the protein A/G-beads were washed with 1 ml of lysis buffer. Subsequently, 20 μL of 2×SDS spiking buffer was added and boiled for 5 min. The protein complexes were incubated with mouse anti-human O-GlcNAcylation (RL2) antibody (1:50). The eluted protein complexes were denatured with 1–5% whole-cell lysate added to SDS loading buffer and heated to 95 °C for 5 min. The protein samples were separated by SDS-PAGE gel and detected by membrane transfer, containment, primary antibody incubation, secondary antibody incubation and development. And analyzed the results of immunoprecipitation.

Western blot (WB)

Proteins were extracted using RIPA lysis buffer and quantified using the BCA method. They were then separated by SDS-PAGE gel electrophoresis and transferred to a polyvinylidene difluoride (PVDF) membrane. After

immersing the membrane in 5% skimmed milk for 2 h at room temperature, appropriate primary antibodies which were rabbit SAPK/JNK (1:1000), rabbit Phospho-SAPK/JNK (1:1000), rabbit p38 MAPK (1:1000), rabbit Phospho-p38 MAPK (1:1000) and mouse GAPDH (1:10000) added and incubated overnight at 4 °C. Membranes followed by incubation with horseradish peroxidase (HRP)-conjugated secondary goat anti-rabbit antibody (1:10000) and goat anti-mouse antibody (1:10000) for 1 h, and visualized by ECL Luminescent Solution AB. The grey scale analysis was performed using ImageJ software (National Institutes of Health, USA).

Statistical analysis

The data were analysed and graphed using Graphpad Prism 9 (GraphPad Software, Inc., USA). All data were expressed as means ± standard deviation (SD). Statistical differences between groups were tested using unpaired two-tailed Student's t-test or One-way test, with $P < 0.05$ considered significant.

Data availability

All data generated or analyzed in this study are included in the present manuscript.

Received: 6 June 2024; Accepted: 21 May 2025
Published online: 29 May 2025

References

1. Javeed, N. & Matveyenko, A. V. Circadian etiology of type 2 diabetes mellitus. *Physiology (Bethesda)* **33**, 138–150 (2018).
2. Shao, Z. et al. Wound microenvironment self-adaptive hydrogel with efficient angiogenesis for promoting diabetic wound healing. *Bioact. Mater.* **20**, 561–573 (2023).
3. Cuadros, D. F. et al. Spatial epidemiology of diabetes: Methods and insights. *World J. Diabetes* **12**, 1042–1056 (2021).
4. Stoekenbroek, R. M. et al. How common are foot problems among individuals with diabetes? Diabetic foot ulcers in the Dutch population. *Diabetologia* **60**, 1271–1275 (2017).
5. Liu, C. et al. Sprayable methacrylic anhydride-modified gelatin hydrogel combined with bionic neutrophils nanoparticles for scar-free wound healing of diabetes mellitus. *Int. J. Biol. Macromol.* **202**, 418–430 (2022).
6. Tian, J. et al. SIRT1 slows the progression of lupus nephritis by regulating the NLRP3 inflammasome through ROS/TRPM2/Ca(2+) channel. *Clin. Exp. Med.* **23**, 3465–3478 (2023).
7. Thiam, H. R. et al. Cellular mechanisms of NETosis. *Annu. Rev. Cell Dev. Biol.* **36**, 191–218 (2020).
8. Gu, Z. et al. Polydatin alleviates severe traumatic brain injury induced acute lung injury by inhibiting S100B mediated NETs formation. *Int. Immunopharmacol.* **98**, 107699 (2021).
9. Lee, K. H. et al. Neutrophil extracellular traps (NETs) in autoimmune diseases: A comprehensive review. *Autoimmun Rev.* **16**, 1160–1173 (2017).
10. Miyoshi, A. et al. Circulating neutrophil extracellular trap levels in well-controlled type 2 diabetes and pathway involved in their formation induced by high-dose glucose. *Pathobiology* **83**, 243–251 (2016).
11. Chatham, J. C., Zhang, J. & Wende, A. R. Role of O-Linked N-Acetylglucosamine protein modification in cellular (patho) physiology. *Physiol. Rev.* **101**, 427–493 (2021).
12. Fan, J., et al., O-GlcNAc transferase in astrocytes modulates depression-related stress susceptibility through glutamatergic synaptic transmission. *J. Clin. Invest.* **133**, (2023).
13. Lee, B. E., Suh, P. G. & Kim, J. I. O-GlcNAcylation in health and neurodegenerative diseases. *Exp. Mol. Med.* **53**, 1674–1682 (2021).
14. Xu, S. et al. Systematic analysis of the impact of phosphorylation and O-GlcNAcylation on protein subcellular localization. *Cell Rep.* **42**, 112796 (2023).
15. Smolle, E. et al. Distribution and prognostic significance of gluconeogenesis and glycolysis in lung cancer. *Mol. Oncol.* **14**, 2853–2867 (2020).
16. Li, D. D. et al. Fungal sensing enhances neutrophil metabolic fitness by regulating antifungal Glut1 activity. *Cell Host. Microbe* **30**, 530-544.e6 (2022).
17. Fadini, G. P. et al. NETosis delays diabetic wound healing in mice and humans. *Diabetes* **65**, 1061–1071 (2016).
18. Wolf, S. J., Melvin, W. J. & Gallagher, K. Macrophage-mediated inflammation in diabetic wound repair. *Semin. Cell Dev. Biol.* **119**, 111–118 (2021).
19. Palsson-McDermott, E. M. et al. Pyruvate kinase M2 regulates Hif-1α activity and IL-1β induction and is a critical determinant of the warburg effect in LPS-activated macrophages. *Cell Metab* **21**, 65–80 (2015).
20. Yang, X. & Qian, K. Protein O-GlcNAcylation: emerging mechanisms and functions. *Nat. Rev. Mol. Cell Biol.* **18**, 452–465 (2017).
21. Chu, Z. et al. Novel neutrophil extracellular trap-related mechanisms in diabetic wounds inspire a promising treatment strategy with hypoxia-challenged small extracellular vesicles. *Bioact. Mater.* **27**, 257–270 (2023).
22. Hart, G. W., Housley, M. P. & Slawson, C. Cycling of O-linked beta-N-acetylglucosamine on nucleocytoplasmic proteins. *Nature* **446**, 1017–1022 (2007).
23. Tadie, J. M. et al. HMGB1 promotes neutrophil extracellular trap formation through interactions with Toll-like receptor 4. *Am. J. Physiol. Lung Cell Mol. Physiol.* **304**, L342–L349 (2013).
24. Kim, S.W. and J.K. Lee, Role of HMGB1 in the interplay between NETosis and thrombosis in ischemic stroke: A review. *Cells* **9** (2020).
25. Balana, A. T. et al. O-GlcNAcylation of high mobility group box 1 (HMGB1) alters Its DNA binding and DNA damage processing activities. *J. Am. Chem. Soc.* **143**, 16030–16040 (2021).
26. Hoste, E. et al. Epithelial HMGB1 delays skin wound healing and drives tumor initiation by priming neutrophils for NET formation. *Cell Rep.* **29**, 2689-2701.e4 (2019).
27. Nyati, K. K. et al. TLR4-induced NF-κB and MAPK signaling regulate the IL-6 mRNA stabilizing protein Arid5a. *Nucleic Acids Res.* **45**, 2687–2703 (2017).
28. Zhou, M. et al. Boosting mTOR-dependent autophagy via upstream TLR4-MyD88-MAPK signalling and downstream NF-κB pathway quenches intestinal inflammation and oxidative stress injury. *EBioMedicine* **35**, 345–360 (2018).

Acknowledgements

Thanks to No.969 Hospital, Joint Logistics Support Force of the Chinese People's Liberation Army for providing the experimental place and equipment and all the participating researchers for their hard work.

Author contributions

Weijing Sun, Jinlong Xu: study design, data analysis, drafting the manuscript and revision of the manuscript.

Shijie Li, Yue Zhao, Jiachen Fu, Lixia Di: data collection and analysis, drafting the manuscript, investigation. Dezhi Han: editing and final approval of the article.

Declarations

Competing interests
The authors declare no competing interests.

Ethical approval
The experimental protocols were approved by The 969th Hospital of the joint logistics support force of P.L.A Laboratory Animal Ethics Committee. All methods were performed in accordance with relevant guidelines and regulations and in accordance with ARRIVE guidelines.

Additional information
Supplementary Information The online version contains supplementary material available at https://doi.org/10.1038/s41598-025-03642-z.

Correspondence and requests for materials should be addressed to D.H.

Reprints and permissions information is available at www.nature.com/reprints.

Publisher's note Springer Nature remains neutral with regard to jurisdictional claims in published maps and institutional affiliations.